

Spatial distribution of heavy metals and Ecological Risk Assessment for the main sub-branches (Rayahs) sediments of Nile River, Egypt

Seliem M. El Sayed

National Institute of Oceanography and Fisheries (NIOF)

Salem G. Salem

National Institute of Oceanography and Fisheries (NIOF)

Mohamed H. Abdo

National Institute of Oceanography and Fisheries (NIOF)

Mohamed H.H. Ali

National Institute of Oceanography and Fisheries (NIOF)

Mohamed E. Goher (✉ smgoher@yahoo.com)

National Institute of Oceanography and Fisheries (NIOF)

Research Article

Keywords: Sediment quality, Rayahs, Nile River, Heavy metals, Pollution indices, Ecological Risk

Posted Date: October 24th, 2022

DOI: <https://doi.org/10.21203/rs.3.rs-1247777/v2>

License: © ⓘ This work is licensed under a Creative Commons Attribution 4.0 International License. [Read Full License](#)

Abstract

Sediments act as a sink or source of pollution under various conditions. Moreover, they can serve as pollution indicators. The present research aims to evaluate sediment quality associated with its content in heavy metals and the potential ecological risk, focusing on the sub-branches of Nile River (Rayahs) in Egypt, including El-Tawfiky (RT), El-Menoufy (RM), El-Behary (RB), and El-Nassery (RN). According to the results, El-Rayahs sediments are characterized by an increasing sand fraction, followed by mud. Regarding heavy metals pollution, Cd registered the highest pollution ranking, whereas Fe, Mn, Zn, Pb, and Ni exhibited the lowest effect. Furthermore, the ecological risk for El-Rayahs sediments increases northward; however, most sites either showed slight pollution or did not record any degree of contamination, except the northern stretch of El-Behary (El-Mahmoudia Canal), which is a very high-polluted zone, with high ecological risk according to the contamination degree (C_d) and potential ecological risk (RI) indices.

Introduction

Sediments are regarded as active substances and dynamic systems, that contain minerals, rocks, sand, and waste of dead animals and plants; they act as a reservoir for organic matter and various pollutants (Goher et al., 2014; Bremner, 2021). Sediments are transported together with heavy elements via adhesion or absorption (Qu et al., 2017). Sediments are also habitat to benthic algae, and invertebrates. Geochemical components and minerals in sediments can indicate the properties, distributions, and sources of pollutants and provide information regarding changes in the aquatic environment and local human activity history (Lan et al., 2011; Yuana et al., 2019). Sediment quality is evaluated by comparing levels of estimated parameters to the regional baseline, historical, and predevelopment (RAMP, 2021). Sediment pollution can occur either directly within water bodies or through transportation by wind, effluents discharge, or rain, carrying heavy elements into the watercourse (Paul, 2017). Heavy metals (HMs), related to human, and/or natural activities, are present in the Earth's environment. HMs pollution is the result of industrialization and urbanization; it is also caused by irrigation water (Ali et al., 2019). Because of their persistence, environmental toxicity, and bioaccumulation, HMs are a major source of pollution in aquatic environments (Huang et al., 2020). In general, water pollution by HMs has become a severe environmental issue in both developing and developed countries because of the progress of civilization, urbanization, and industrialization, leading to the discharge of massive amounts of untreated wastes into the aquatic ecosystem (UNCSD, 2010; Arefin, 2016; Goher et al., 2019). According to Mateo-Sagasta et al., (2017), irrigation water represents about 70% of water abstractions worldwide, making agricultural wastes an important source of contamination of the aquatic environment (Goher et al., 2019). Further, more than 80% of the global municipal wastewater is flowing into watercourses without treatment, as set by WWAP (2017).

In watercourses and riverine systems, HMs are considerably more concentrated in sediments than in the water body, and most HMs immediately deposit after entering rivers (Shyleshchandran et al., 2018). Under suitable hydrological and chemical conditions, HMs can be released into the water column, causing the watercourses pollution and affecting the health of aquatic organisms (Kouidri et al., 2016). Furthermore, HMs accumulation in sediments directly affects the benthic creatures, as well as other organisms through the food web (Fu et al., 2014; Huang et al., 2020). Therefore, it is of great importance to study the distribution and levels of HMs in sediments of rivers, waterways, and all water bodies, in addition to assessing the potential environmental risk of HMs.

The Nile River represents the soul of Egyptians, providing them approximately 95% of freshwater used by them. Weathering of the rocks of the Ethiopian Highlands led to the enrichment of sediments of the Nile River with elements such as Fe, Mn, Cu, Cr, and Ni (Elnazer et al., 2018; Mostafa et al., 2019). After constructing the High Dam in Aswan, the largest portion of these metals is deposited in the southern part of Nasser Lake (Imam et al., 2020; Goher et al., 2021). However, as a result of the increase in population and industrial enhancement, Nile receives huge amounts of different wastes, inorganic and organic pollutants, and HMs through its traveling into the Mediterranean Sea through Sudan and Egypt (Goher et al., 2019, 2021). At El-Delta Barrage in Egypt, Nile bifurcates into two main branches, Damietta and Rosetta, and four other canals or sub-branches (called Rayah). The four Rayahs, from east to west, are El-Tawfiky (RT), El-Menoufy (RM), El-Behary (RB), and El-Nassery (RN) (Goher, 2015; Talab et al., 2016; Goher et al., 2021). Rayahs, in addition to Rosetta and Damietta branches, provide freshwater for various purposes to approximately 40 million capita in the Delta region and Alexandria Governorate (Goher, 2015).

The aim of this study is to evaluate the sediment quality of the Rayahs and El-Mahmoudia and El-Nubaria Canals, in terms of HMs content and the effect of environmental conditions on their distribution pattern. Ecological risk indices were used to study sediment pollution using different assessment approaches.

Material And Methods

Study Area

After traveling for approximately 950 km from Aswan in the south to Cairo in the north, Nile River bifurcates in two branches, Rosetta and Damietta, at 1.5-km southern El-Kanatieh El-Khyeria, where RM, RB, and RN originate from the former and RT originates from the latter (Fig. 1). El-Rayahs are characterized by the existence of several water treatment (most are small stations), electric power plants, and villages, Ezzabs (small villages), and small towns, heavily scattered on both sides. The El-Rayahs' lengths extend from approximately 180 km (RM) to 215 km (RB), with an average width of 40–50 m and an average depth of 2–5 m. The water levels in all El-Rayahs decrease downstream; therefore, they are replenished again with water from Damietta (RT and RM), Rosetta (RB), and RN (RN). A severe shortage of water and a noticeable drop in water level occurs at the end of these Rayahs, except for RN, which is an important navigable stream.

RT arises from Damietta branch and extends into the middle and eastern part of the Delta, heading north, parallel to some extent with Damietta branch until Mansoura City at T5, where it branches into two parts: the first is heading north to Damietta City, and is characterized by a lack of water and narrow width; almost all water disappears at Faraskour City, thus water samples are not collected from this branch. The second, which is characterized by abundant water respect to the first, runs eastward within Dakahlia Governorate, across Dekerness, El-Gamalia, and El-Manzalah cities. In the past, this branch flowed into Manzalah Lake. Before station T5, the El-Rayah is refilled with freshwater from the Damietta branch.

RM starts from Rosetta branch at El-Kanater El-Khayria City and extends into the middle part of the Delta, thus breaking El-Menoufia, El-Dakahlia, and El-Gharbia Governorates, then heading north to Gamasa City and the southern part of Burullus Lake; this Rayah has a high number of minor branches, particularly in the El-Menoufia Governorate. At Zifta City (upstream of site M5), a connected canal bearing large quantities of water from Damietta branch discharges water into RM, to increase the water level, which decreases gradually again.

RB originates from Rosetta branch at El-Kanater El-Khayria City and stretches into the western part of the Delta in a NW direction, parallel to the Rosetta branch and west of Giza Governorate through Nikla, Abu-Ghalib, and El-Khatatba cities. Next, it passes Beheira Governorate through Kafr-Daoud, Kom-Hamada, Itai El-Baroud, Damanhur, Kafr El-Dawar cities, and Alexandria Governorate. Notably, RB crosses with El-Mahmoudia Canal after Damanhur City (El-Mahmoudia Canal originates from Rosetta branch at El-Mahmoudia City). This segment (from sites B6-B9) flows northwest until Alexandria, where it is named El-Mahmoudia Canal.

RN begins from Rosetta branch at El-Kanater El-Khayria City and runs in the western part of the Delta, parallel to RB, where it flows northwest toward the Noubaria Canal that originates from RB. RN joins El-Nubaria Canal, near Kanater Pauline (at Koum Hamada), before traveling northwest across Mariout Lake, to end at the Mediterranean Sea. The segment from sites N4 to N8 is named El-Nubaria Canal.

Sampling

A total of 31 surface sediment samples (including 7 from RT, 7 from RM, 9 from RB, and 8 from RN) were collected in late 2017 (Table 1). Samples were sealed in airtight polythene bags as promptly as possible. Hence, sediments were dried in drying Oven at 105 °C to a consistent weight and were ground using a mortar and pestle. Later, samples were sieved to < 120 µm.

Table 1
Details and description of the selected sites of the study area

Site	Name	Latitude	Longitude	Distance (km)*	Description
T1	El Kanater	30°11'46.58"	31° 7'55.98"	1-1.5	/very fast water /receives few wastewater
T2	Banha	30°28'24.0"	31°12'1.04"	35	opposite of Benha water plant /residential region in the two sides
T3	Met-Ghamr	30°41'35.3"	31°16'50.2"	65	It flows Between agricultural and residential regions beside the agricultural way (Cairo-El-Mansoura)/
T4	Agga	30°54'23.12"	31°16'51.88"	90	It flows Between agricultural and residential regions in the two sides
T5	Mansoura	31°04'02.84"	31°25'02.13"	115	Before branching of El-Rayah/ Between agricultural and residential regions
T6	Dekerness	31° 5'38.65"	31°37'37.77"	130	Residential region in the west side and agricultural region in east side/low water level
T7	El-Manzalah	31°09'49.9"	31°56'09.5"	170	Static water/ receives a lot of wastes
M1	El Kanater	30°11'59.85"	31° 6'44.97"	1	Downstream the Delta Barrage/receives few wastewater
M2	El-Khadra	30°20'15"	31° 02'55"	30	It is between agricultural and residential regions
M3	Shebeen El-Koum	30°32'04.3"	31°00'48.3"	60	It is between agricultural and residential regions
M4	El-Santa	30°43'44.50"	31° 7'28.88"	85	Receives large amount of wastewater with slow water current
M5	Zifta	30°47'26.15"	31° 9'16.12"	95	Downstream the replenishing with water from Damietta branch
M6	El-Mahalla	30°56'59.4"	31°09'21.4"	115	Between residential regions / receives few wastewater
M7	Belqas	31°07'59.9"	31°22'50.1"	155	Between agricultural regions
B1	El Kanater	30°10'47.36"	31° 6'18.69"	3-4	It runs between agricultural and industrial regions / receives few wastewater
B2	Abo ghaleb	30°14'46.90"	30°56'33.68"	30	Downstream Abu-ghaleb electrical plant/ agricultural region in east side
B3	Kafr Dawood	30°27'3.75"	30°49'41.35"	60	It flows between agricultural and residential regions
B4	El-Tawfikia	30°48'36.91"	30°45'21.65"	100	at El-Tawfikia bridge/ beside agricultural way (Cairo-Alexandria)
B5	Damanhour 1	31°00'46.5"	30°28'52.8"	135	At the entrance of Damanhour city
B6	El-Mahmoudia	31°10'25.9"	30°31'42.1"	145	1 Km downstream the originate of El-Mahmoudia Canal from the Rosetta branch
B7	Damanhour 2	31° 5'16.85"	30°25'16.79"	140	Downstream the confluence of RB with El-Mahamoudia /Middle of a crowded residential region
B8	Kaffr El-dawar	31° 7'31.58"	30°13'31.82"	170	Between agricultural and residential regions at the two sides/Low water level
B9	El-Siuof	31°13'6.67"	29°59'39.74"	205	Upstream the end of El-Rayah/ Next to many of water and electricity plants/Low water level
N1	El Kanater	30°10'36.78"	31° 6'29.77"	2	Between residential regions
N2	El-Khatatba	30°19'57.76"	30°48'57.5"	40	Between agricultural and residential regions
N3	Koum Hamada	30°30'31.3"	30°48'18.6"	70	Located before the confluence of El-Rayah with El-Nubaria Canal / surrounded by agricultural regions
N4	El-Noubaria 1	30°42'51.0"	30°44'26.8"	93	The beginning of El-Nubaria Canal / very fast water flow
N5	El-Noubaria 2	30°43'44.69"	30°33'47.14"	90	It receives wastes of Kom Hamada electricity plant/ downstream meeting of El-Rayah with El-Nubaria Canal
N6	Itai El-Baroud	30°49'4.75"	30°14'57.56"	115	Between agricultural and residential regions
N7	Housh-Issa	30°54'38.06"	30° 2'9.52"	140	Between agricultural and residential regions
N8	El-Haouies	30°59'54.76"	29°51'49.97"	190	Before El-Nubaria current lock (El-Haouies)

* Distance downstream of the Delta Barrage

Procedures

Grain size analysis and sediment textural classes were performed according to (Folk, 1980). Methods by (Griffiths, 1951) and (Carver, 1971) were used to analyze samples with > 5% fine fraction (finer than 40). Organic matter (OM) was determined by loss on ignition (Hanna, 1965).

As described by (Goher et al., 2021), microwave digestion of sediments was performed according to the USEPA 3052 method (USEPA, 1996a). The studied metals (Fe, Mn, Zn, Cu, Cr, Ni, Pb, and Cd) were analyzed using inductively-coupled argon plasma atomic absorption (ICP 6500 Duo, Thermo Scientific, England).

Pollution index

Seven pollution indices were used to assess the ecological risk of the four Rayahs sediments, including contamination factor (CF), contamination degree (C_d), pollution load index (PLI), ecological risk factor (Er), potential ecological risk index (RI), enrichment factor (EF), and index of geo-accumulation (Igeo). CF, Er, EF, and Igeo are single indices, whereas C_d , PLI, and RI represent integrated indices (Table 2).

In the present study, average shale values (ASVs), reported by (Turekian & Wedepohl, 1961), were used as a reference level of HMs, instead of background values. ASVs of the studied metals are 46700, 950, 95, 40, 20, 68, 90, and 0.3 $\mu\text{g/g}$ for Fe, Mn, Zn, Cu, Pb, Ni, Cr, and Cd, respectively.

Table 2
Pollution classes of indices used.

Single Indices								
EFclasses ¹		CFclasses ²		Igeo classes ³		Er classes ²		
Efvalue	Pollution	Cfvalue	Pollution	Igeo	Igeo class	Pollution	value	Ecological Risk
EF < 2	Depletion to mineral	CF < 1	Low	< 0-0	0	Unpolluted	< 40	Low
2 ≤ EF ≤ 5	Moderate	1 ≤ CF ≤ P ₃	Moderated	0-1	1	Unpolluted to moderated	40 < Er < 80	Moderated
5 ≤ EF ≤ 20	Significant	3 ≤ CF ≤ 6	Considerable	1-2	2	Moderated polluted	80 < Er < 160	Considerable
20 ≤ EF ≤ 40	Very high	CF > 6	Very high	2-3	3	Moderated to high polluted	160 < Er < 320	high
EF > 40	Extremely high			3-4	4	Highly polluted	Er > 320	Very high
				4-5	5	Highly to extremely polluted		
				5-6	> 5	Extremely polluted		
Integrated Indices								
C_d Classes ²		PLI ⁴		RI classes ²				
C_d value	Pollution	value	Pollution	Rvalue	Ecological Risk			
$C_d < m$	Low	0	Perfection	RI < 150	Low			
$m < C_d < 2m$	Moderated	< 1	Baseline levels	150 < RI < 300	Moderate			
$2m < C_d < 4m$	Considerable	> 1	Polluted	300 < RI < 600	Considerable			
$C_d > 4m$	Very high			RI > 600	Very High			
¹ Sutherland (2000); ² Hakanson (1980); ³ Muller(1981); ⁴ Tomlinson et al., (1980).								

Contamination factor

The level of contamination of sediments by given toxic substances (metals), suggested by (Hakanson, 1980), is expressed in terms of a contamination factor (CF) and is calculated as

$$CF = \text{metal content in the sediment} / \text{background level of metal. (1)}$$

Contamination degree

The degree of contamination (C_d) was originally defined as the sum of all contamination factors: (C_d) = $\sum CF$ (2).

The pollution load index

Tomlinson et al., (1980) proposed the pollution load index (PLI). PLI for a single site is the n^{th} root of the product of n CF values, according to the following formula:

$$PLI \text{ for a site} = \sqrt[n]{CF_1 * CF_2 * \dots * F_n} \text{ (3)}$$

where CF = contamination factor and n = number of metals, whereas

$$PLI \text{ for a zone} = \sqrt[n]{\text{site}_1 * \text{site}_2 * \dots * \text{site}_n} \text{ (4)}$$

where n equals the number of sites.

Ecological risk factor and Potential ecological risk

An ecological risk factor (Er) is a numerical expression of a contaminant's potential ecological risk:

$$Er = T * CF, (5)$$

where T is the toxic response factor for a specific substance and CF is the contamination factor. T equals 1 for Fe, Mn, and Zn; 2 for Cr; 5 for Cu, Pb, and Ni; and 30 for Cd (Hakanson, 1980). In the same context, the potential ecological risk (RI), which is defined as the sum of risk factor

$$RI = \sum Er (6)$$

Enrichment factor

The EF is a commonly used method for determining enrichment ratios and the degree of anthropogenic pollution (Zakir et al., 2008):

$$EF = [C_M/C_X]_{\text{sample}} / [C_M/C_X]_{\text{Earth's crust}} (7)$$

where C_M is the concentration of the analyzed metal and C_X is the concentration of the immobile element, such as Al, Fe, Ti, Mn, Li, Sc, or Zr (Blaser et al., 2000; Liu et al., 2005; Chatterjee et al., 2007; Zhang et al., 2007; Goher et al., 2014; Tiomo et al., 2021).

Geo-accumulation index

The geo-accumulation index (I_{geo}) values are calculated for the studied metals introduced by Muller (1981), as follows:

$$I_{geo} = \log_2 [C_n / (1.5 * b_n)] (8)$$

where C_n is the content of analyzed element (n) in the sample and b_n is the geochemical background.

Results And Discussion

Grain size, moisture, and organic matter analysis

Sediment fractions, moisture, and organic matter (OM) contents of the Rayahs sediment are given in Table 3. Sand was the dominant fraction, varying in the ranges of 42.79%-73.84%, 27.73%-87.77%, 36.74%-82.23%, and 19.23%-84.20% in RT, RM, RB, and RN, respectively (Table 3 and Fig. 2). Sand was deposited through erosion of two banks and by wind (aeolian deposits, with fine to very-fine sand) with limited water movement. RB and RT were characterized by low sand deposition compared to RN and RM. Sand fraction exhibits a strong negative correlation with mud ($r = -78$), moisture % ($r = -53$; $p = 0.01$), and Fe ($r = -0.4$; $P < 0.05$). This is related to silt and fine-grained clays that reflect sedimentation during commonly-occurring perennial water flows and coarse-grained clastic layers in between this clay matrix; therefore, they reflect a very high energy environment, or flood events (Raja et al., 2018).

By contrast, the main gravel fractions were in the range of 0.5%-47.24%, 0.26%-12.40%, 2.56%-24.01%, and 1.7%-20.59% in RT, RM, RB, and RN, respectively, with an order of $RT > RB > RN > RM$. (Table 3 and Fig. 2). Notably, gravel fraction comprised mollusca shells and fragments associated with granules deposited by banks erosion and some gravel > 2 mm was transported to sub-branches by human activity at banks.

Mud fraction is the second dominant after sand in the ranges of 9.97%-48.11% (average 28.39%) for RT, 9.72%-65.43% (average 36.62%) for RM, 12.38%-46.36% (average of 28.98%) for RB, and 6.53%-60.17% (average 28.79%) for RN. Rate of mud deposition increased northward, related to the decrease of water movement. Mud (silt and clay) was deposited via water (river deposit) and wind (aeolian deposits) from the two banks. The results agreed with those obtained by Abu El-Enain et al., (1997); Abd El-Monsif (2009); Salem and Lotfy (2017); Goher et al., (2021), who stated that the dominant fractions of Nile River are sand $>$ mud (silt and clay) $>$ gravel. We can state that the distribution of grain size depends on the depth and energy of water movement, where mud (clay and silt) increased with depth and quite water with slow currents, while sand and gravel increased at banks with low depth and high movement water. After the establishment of the Aswan High Dam in 1964, great changes in the hydrological system in the Nile Delta led to a halt in the arrival of sediments and floodwaters to the Mediterranean Sea. The sources of sediments in the Nile River are the shore erosion and aeolian sedimentation (Stanley et al., 2004; Hamouda et al., 2014; Ghoneim et al., 2015; Elsherif et al., 2020; Goher et al., 2021). Mud exhibits a strong positive correlation with moisture % ($r = 0.73$, $n = 31$; $p < 0.01$) and OM% ($r = 0.043$; $n = 31$; $p < 0.05$); this can be related to the fermentation process, which is conducted through the sinking of dead microorganisms forming organic matter (Dinakaran & Krishnaya, 2011; Farahat, 2019).

OM in sediments is the remains of organic life, fossils in the geological sense (Welte, 1696). Numerous indicators, or proxies, can be derived from the OM composition of sediments and used to reconstruct the paleoenvironments of water bodies and their watersheds (Dianto et al., 2020). Regarding the obtained results, the horizontal distribution of OM is shown in Table 3 and Fig. 3. OM contents in the Rayahs sediments were found in the order of $RN < RB < RM < RT$, with mean values of 8.12%, 8.55%, 10.57%, and 11.17%, respectively (Table 3 and Fig. 3). We found that OM percentage increases with mud fraction with respect to sand and gravel fractions, which is consistent with the results obtained by Salem, (2011); Goher et al., (2021). Results showed the increase of the OM in RM and RT with respect to RB and RN, which may be related to the high population, and thus, human activity, in the first two Rayahs. OM showed a strong positive correlation with moisture % ($r = 0.5$; $n = 31$; $p < 0.01$) that may be explained by the high porosity of mud, which stores OM and water.

Water content is one of the most important indicator properties used to establish a correlation between sediment behavior and its indicator properties. Moisture percentage has been defined as the ability of sediment to save water. Moisture contents in sediments varied in the ranges of 40.23%-64.98%,

38.93%-72.30%, 38.91%-63.42%, and 36.53%-71.28% in RT, RM, RB, and RN, respectively (Table 3 and Fig. 3). RM Sediment has a higher moisture content followed by RN, whereas RT and RB show low values.

Table (3): Texture and heavy metal contents in the four Rayahs sediments.

parameter	El-Tawfiky				El-Menoufy				El-Beahy				El-Nassery			
	Min	Max	Av	Sd	Min	Max	Av	Sd	Min	Max	Av	Sd	Min	Max	Av	
Gravel	0.57	47.24	15.01	± 17.4	0.26	12.40	5.09	± 4.69	2.56	24.01	9.93	± 6.64	1.70	20.59	9.09	
Sand	42.79	73.84	56.62	± 9.7	27.73	87.77	56.64	± 19.4	36.74	82.24	60.86	± 15.1	19.24	84.20	62.11	
Mud	9.97	48.11	28.39	± 14.2	9.72	65.43	36.62	± 19.5	12.38	46.36	28.98	± 13.0	6.53	60.17	28.79	
Mo%	40.23	64.98	49.65	± 9.27	38.93	72.30	54.68	± 12.1	38.91	63.42	49.92	± 8.81	36.53	71.28	52.97	
O.M%	5.87	16.47	11.17	± 4.12	6.82	15.75	10.57	± 3.38	4.48	14.15	8.55	± 3.51	4.78	14.08	8.12	
Fe mg/g	6.75	6.75	10.51	± 2.62	7.91	13.61	10.42	± 2.10	7.12	14.90	10.58	± 2.95	7.36	12.13	9.69	
Mn µg/g	123.2	201.8	153.85	± 25.9	177.2	252.0	199.83	± 26.1	239.14	422.50	316.07	± 66.6	165.29	245.96	198.69	
Zn µg/g	16.38	36.36	23.75	± 7.33	20.80	41.66	29.33	± 7.09	7.12	109.56	82.50	± 16.6	26.33	48.93	39.08	
Cu µg/g	4.96	12.68	8.76	± 2.46	9.51	16.51	12.57	± 2.39	20.02	40.05	28.39	± 7.18	14.68	23.66	18.47	
Pb µg/g	4.82	12.90	7.81	± 2.49	7.06	15.90	10.20	± 3.29	8.14	27.54	15.61	± 7.90	8.11	18.60	12.43	
Ni µg/g	3.22	5.62	4.07	± 0.87	3.08	6.78	4.38	± 1.20	2.38	8.54	4.83	± 2.23	2.63	8.57	5.10	
Cr µg/g	3.35	8.79	5.98	± 1.70	6.28	11.08	7.84	± 1.57	10.70	33.50	21.03	± 7.79	6.61	16.54	11.62	
Cd µg/g	0.42	1.27	0.703	± 0.28	0.72	1.14	0.91	± 0.18	0.785	3.07	1.62	± 0.84	0.722	1.39	1.09	

Heavy Metals

Sediment contamination poses one of the worst environmental threats in ecosystems, which act as sinks and sources of contaminants in aquatic systems; thus, sediment analysis is critical for assessing the pollution status of the environment (Mucha et al., 2003). Geochemical analyses of Fe, Mn, Zn, Pb, Cu, Ni, Cr, and Cd were conducted, and their concentrations are listed in Table 3 and represented in Fig. 4.

Iron (Fe) is one of the major constituents of the lithosphere; it is critical in the behavior of several trace elements and is located in the intermediate position between macro and micronutrients in plants, animals, and humans (Kabata-Pendias & Arun, 2007). The sediment content in Fe is controlled by several factors, including the distance from the outfall, nature of sediment, OM content, oxidation/reduction conditions, TDS levels (salinity), and pH value of water (Masoud et al., 2011; Goher et al., 2021). Concerning our results, the lowest (6.75 mg/g) and the highest (15.17 mg/g) values of Fe were recorded in RT at sites T1 and T7, respectively, which is consistent with the results obtained by Goher et al., (2021), who worked in River Nile. However, our results are lower than those regarding Ismailia Canal, Rosetta branch, and Greater Cairo, obtained by El Sayed (2015); El-Amier et al., (2015); Lasheen and Ammar (2009). Fe exhibits a strong positive correlation ($n = 31$; $p < 0.01$) with Mn ($r = 0.47$), Pb ($r = 0.72$), Ni ($r = 0.67$), Cr ($r = 0.47$), and Cd ($r = 0.69$) and is positively correlated ($n = 31$; $p < 0.05$) with Zn ($r = 0.36$) and Cu ($r = 0.40$), indicating the common source and association of metals with oxy-hydroxides of Fe-Mn, which is also supported by Imam et al., (2020); Goher et al., (2021). Furthermore, the positive correlation of Fe with OM ($r = 40$, $n = 31$; $p < 0.05$) indicates the association of Fe deposition with OM accumulation in the sediment.

Manganese (Mn) exists in sediments principally as MnO_2 , which is very insoluble in water under reducing conditions: Mn in the dioxide form is reduced from valence 4 to 2, and solubility occurs as with ferric oxide (Ahmed et al., 2019). Mn shows irregular distribution patterns in all Rayahs sediments; the lowest value (123.16 µg/g) has been found in RT and the maximum (422.5 µg/g) in RB, with a major difference between sites. This result was lower than that obtained in previous studies in Greater Cairo (Lasheen and Ammar 2009), Rosetta branch (El Bouraie et al., 2010), and Nasser Lake (Imam et al., 2020). The strong positive correlation ($n = 31$; $p < 0.01$) of Mn with Zn ($r = 0.95$), Cu ($r = 0.95$), Pb ($r = 0.84$), Ni ($r = 0.57$), Cr ($r = 0.96$), and Cd ($r = 0.89$) indicates that it probably represents the geochemical support phases of these metals, associated with Mn coprecipitate, adsorbed on Mn oxides, or hydroxide (Ottosen et al., 2006).

Zinc (Zn) may occur in sediments as carbonate, oxide, and sulfide (AIP, 2017; Imam et al., 2020); its concentration is mainly attributed to the input of organic wastes in aquatic environments, which come from municipal sewage and dumping materials, in addition to industrial discharges, sewage effluent, and runoff

sources (Alagarsamy, 2006; Goher et al., 2015). In the present study, Zn content ranged between 16.38 µg/g (in RT) and 109.56 µg/g (in RB), with a high spatial significant difference ($p < 0.01$) based on ANOVA data. These findings may be related to the anthropogenic at the ends of the rayahs especially in RB. The obtained results were lower than the corresponding values found in River Nile (102.2–261 µg/g) (Abdel-Satar, 2005), Damietta branch (75.5–888.5 µg/g) (Goher, 1998), and Upper Egypt (1–271 µg/g, with an average of 114 µg/g) (El-Kammar et al., 2009). However, values were higher than that recorded in Nasser Lake (11.55–82.71 µg/g) (Imam et al., 2020) and close to the values ranging from 10 to 145.95 µg/g in Ismailia Canal, obtained by El Sayed (2015) and in Greater Cairo (Lasheen and Ammar 2009). Zn exhibits a strong positive correlation ($n = 31$; $p < 0.01$) with Cu ($r = 0.95$), Pb ($r = 0.74$), Cr ($r = 0.92$), Cd ($r = 0.82$), and Ni ($r = 0.43$, $n = 31$; $p < 0.05$).

Figure (4): Box plot of the studied trace metals in the sediment of the four Rayahs.

Copper (Cu) is a micronutrient element fundamental to all forms of life. In excessive amounts, it may become toxic to organisms by inducing a reduction in enzymes activity or a random rearrangement of structural proteins (Goldman, 2009; Karak et al., 2017; Goher et al., 2019). The high Cu concentrations in El-Rayahs sediments may be attributed to the high accumulation of OM and Fe-Mn oxy-hydroxides produce simultaneous accumulation of HMs in sediments (Ottosen et al., 2006). The highest value (40.05 µg/g) of Cu was recorded in RB and the lowest (4.96 µg/g) in RT, with considerable difference between locations. The obtained results were lower than the corresponding values in River Nile (average, 42 µg/g) (El-Kammar et al., 2009) and Greater Cairo 27–90 µg/g (Lasheen & Ammar 2009). However, values were close to those (1.0–40.3 µg/g) obtained by Imam et al., (2020) for Nasser Lake. Cu exhibits a strong positive correlation ($n = 31$; $p < 0.01$) with Pb ($r = 0.84$), Cr ($r = 0.97$), Cd ($r = 0.88$), and Ni ($r = 0.56$); these results are consistent with the several studies (Goher et al., 2014; El Sayed, 2015; Goher et al., 2021; Abou El-Anwar et al., 2021), who reported that the deposition of Cu and Zn is enhanced by the association of metals with clay minerals or the adsorption of both elements on hydrated iron and manganese oxides. These authors also added that the order of adsorption of most mobile metals fraction is Fe/Mn oxides > OM > clay.

Lead (Pb) is considered as one of the most toxic elements to humans and animals, and its toxicity is largely dependent on its solubility (Wani et al., 2015); the form of $PbSO_4$ is much soluble than $PbCO_3$ and has a greater toxicity, whereas PbS has a very low solubility and toxicity (Lide, 2008; SCDHEC, 2020). Pb enters the aquatic environment throughout precipitation of dust fall out, leaching soil, and industrial wastes discharge (Abd El-Aal 2020). Pb contents varied in the range of 4.82–27.54 µg/g in RT and RB, respectively; this result is consistent with the results obtained by (Mostafa et al., 2019) for River Nile and (Goher et al., 2014) for Nasser Lake, whereas they are higher than those obtained by Lasheen and Ammar (2009) for Nile River in Greater Cairo (2.33–7.5 µg/g) and lower than those of Upper Egypt (average, 10 µg/g) obtained by El-Kammar et al., (2009). Pb has a strong positive correlation ($n = 31$; $p < 0.01$) with Ni ($r = 0.84$), Cr ($r = 0.87$), and Cd ($r = 0.95$).

Nickel often was considered an essential nutrient for animals. Now, Ni is generally not classified an essential element for humans and higher animals (Nielsen, 2021). Oppositely, Ni is possibly harmful and poisonous to aquatic organisms and is listed in the priority elements for the water quality field within the European Union of Water Framework Directive (Szarek-Gwiazda et al., 2011). In general, the pentlandite is the primary nickel source. Ni may be found in basalt, sandstone, slate, and clay minerals. It accumulates in sediments and is a part of various biological cycles. Nickel may enter lakes, rivers, and streams from non-point and point sources, such as emissions of metal industries, waste incinerators, and power plants. Moreover, Ni is directly discharged to water bodies from various industries (Lenntech, 2022).

In the present study, the maximum (8.57 µg/g) and minimum (2.38 µg/g) values of Ni were recorded at RN and RB, respectively; they are lower than the range of 59–65 µg/g found for Greater Cairo by Lasheen and Ammar (2009), from the value of 28.56 µg/g obtained by El Sayed (2015) for Ismailia Canal, and the range of 5.2–40 µg/g obtained by Goher et al., (2021) for River Nile. Ni has a strong positive correlation ($n = 31$; $p < 0.01$) with Cr ($r = 0.61$) and Cd ($r = 0.73$).

Chromium (Cr) is a transition metal, found in water in oxidation states, ranging from Cr^{+6} to Cr^{-2} ; it is a nonessential element and is classified as a toxic metal, entering watercourses through both anthropogenic and natural sources, such as geogenic processes and interaction of microbes with mafic and ultramafic rocks, in addition to industrial activities, such as production of energy, chemicals, and metals manufacturing. Furthermore, different wastes release Cr compounds into the aquatic environment (Tumolo et al., 2020). Concerning our results, the highest value of Cr (33.5 µg/g) was recorded at RB, whereas the lowest (3.45 µg/g) was recorded at RT with highly significant difference between sites. These values are lower than 185.6 µg/g, obtained by El Bourie et al., (2010) for Rosetta branch and higher than the range of 0–8.5 µg/g, obtained by Goher et al., (2021) along the River Nile, from Aswan to Cairo. On the contrary, our results are close to the 36.6–46 µg/g range found for Greater Cairo by Lasheen and Ammar (2009). Chromium has a strong positive correlation with Cd ($r = 0.91$, $n = 31$, $p < 0.01$).

Cadmium (Cd) precipitates as $CdCO_3$ coprecipitation, which is similar to lead (Imam et al., 2020; Goher et al., 2021). Its content showed a maximum level (3.066 µg/g) at RB, whereas the lowest (0.421 µg/g) was recorded at RT, with highly significant difference between sites; these results were lower than the corresponding values in River Nile in Upper Egypt (average of 3 µg/g) and Damietta branch (2.04–36.64 µg/g), according to (El-Kammar et al., 2009; Goher, 1998), respectively. However, our values are close to the ranges of 0.1–4.3 µg/g and 1.7–3 µg/g, obtained by Lasheen and Ammar (2009) in Greater Cairo and El Sayed (2015) for Ismailia Canal, respectively.

Notably, the maximum values for most metals, based on mean values, have been found at RB (except for nickel at RN), whereas minimum values (on average) were recorded at RT. Furthermore, the increase of HMs in the northward sediments among all Rayahs is attributed to the impact of human activities along their sides. The data of Pearson's correlation coefficients between the measured metals with Fe and Mn ($r = 0.47–0.98$, $n = 31$, $p < 0.01$) revealed the role of steeling of Fe and Mn oxides in the deposition of metals into the sediment. In the same context, the positive correlation of metals with organic matter demonstrated the relation between OM accumulation and the distribution of HMs in sediments. The present study confirmed that the order of deposition of most metals is associated with Fe and Mn oxides > OM > clay, which is consistent with the results obtained by Ottosen et al., (2006); El-Kammar et al., (2009); Goher et al., (2014); Goher et al., (2021); Abou El-Anwar et al., (2021).

Ecological risk indices

different approaches have been established for the assessment of HM risk in sediment. Where, there are many pollution indices widely used to assess the environmental risk of the sediment, The indices may be single, such as (contamination factor (CF), enrichment factor (EF), ecological risk factor (Er), and index of geo-accumulation (Igeo), or integrated indices, as pollution load index (PLI), potential ecological risk index (RI), and contamination degree (Cd). (Goher et al., 2021). In general, single indices are interested to assess the potential risk for each individual HM, while the integrated indices take into account all possible risks for a group of HMs. The management of environmental risk management supplies policymakers, resource managers, and the public with regular methods that enable informed decision-making (Goher et al., 2014).

Contamination factor

The level of contamination of El-Rayahs sediments by given toxic substances is expressed in terms of a contamination factor (CF), The pollution grade of sediments, according to CF values, is given in Table 4. The most studied metals exhibited low contamination for all samples, except Cu, that exhibited moderate contamination at site B6 in RB. However, the contamination factors of Cd exhibited spatial variation, changing from moderate in most sites to very high at site B6 in RB.

Contamination degree

Regarding the rayahs sediments, results showed that the degree of contamination (C_d) was low at all Rayahs, except the northern part of RB (El-Mahmoudia Canal), which was very-highly contaminated (Table 4).

The pollution load index

PLI can provide useful information on the level of pollution at a given location (Mohiuddin et al., 2010; **Harikumar & Jisha, 2010**). PLI data (Table 4) provide a simple comparison mean for evaluating the quality of a site or area (0.0 denotes perfection, 1.0 indicates the baseline levels of existent contaminant, and > 1.0 indicates tolerant deterioration of the site) (Table 2) (Tomlinson et al., 1980; **Cabrera et al., 1999**). Based on PLI values of El-Rayahs sediments, which are < 1 in all examined sites, they are categorized as not significantly polluted.

Table (4): Contamination factor, Degree of Contamination (Cd) and Pollution Load Index (PLI) of the studied trace metals of the four Rayahs sediments.

Site	Contamination Factor (Cf)								Degree of Contamination (Cd)	Pollution Load Index (PLI)
	Fe	Mn	Zn	Cu	Pb	Ni	Cr	Cd		
T1	0.144	0.130	0.172	0.124	0.241	0.052	0.037	1.404	2.305	0.151
T2	0.184	0.145	0.179	0.176	0.322	0.050	0.054	1.640	2.750	0.182
T3	0.210	0.144	0.183	0.207	0.367	0.047	0.063	1.93	3.151	0.199
T4	0.241	0.164	0.266	0.218	0.389	0.071	0.078	2.303	3.730	0.241
T5	0.229	0.178	0.273	0.228	0.372	0.062	0.067	2.474	3.882	0.236
T6	0.243	0.160	0.293	0.263	0.397	0.054	0.069	2.447	3.925	0.239
T7	0.325	0.212	0.383	0.317	0.645	0.083	0.098	4.215	6.277	0.341
zone										0.221
M1	0.169	0.187	0.257	0.238	0.374	0.053	0.074	2.453	3.806	0.227
M2	0.174	0.205	0.219	0.246	0.353	0.056	0.070	2.412	3.735	0.225
M3	0.194	0.187	0.247	0.306	0.395	0.045	0.081	2.470	3.924	0.236
M4	0.291	0.265	0.439	0.413	0.795	0.100	0.123	3.813	6.239	0.389
M5	0.245	0.220	0.320	0.325	0.460	0.065	0.085	3.291	5.012	0.288
M6	0.248	0.194	0.336	0.332	0.540	0.060	0.087	3.308	5.105	0.290
M7	0.239	0.214	0.343	0.340	0.654	0.071	0.090	3.577	5.529	0.312
zone										0.276
B1	0.167	0.299	0.702	0.541	0.518	0.057	0.186	2.615	5.084	0.358
B2	0.153	0.268	0.828	0.583	0.421	0.041	0.154	3.383	5.832	0.340
B3	0.177	0.267	0.762	0.500	0.407	0.035	0.157	3.363	5.670	0.329
B4	0.209	0.252	0.748	0.565	0.503	0.045	0.119	3.582	6.022	0.348
B5	0.176	0.307	0.666	0.660	0.448	0.050	0.228	3.346	5.880	0.377
B6	0.319	0.445	1.153	1.001	1.377	0.126	0.372	10.220	15.014	0.757
B7	0.276	0.378	0.886	0.808	1.062	0.086	0.283	7.738	11.516	0.591
B8	0.266	0.363	0.956	0.822	1.037	0.092	0.276	5.759	9.571	0.572
B9	0.298	0.416	1.114	0.907	1.252	0.108	0.328	8.509	12.932	0.683
zone										0.368
N1	0.182	0.198	0.417	0.420	0.405	0.064	0.106	2.815	4.606	0.289
N2	0.181	0.192	0.359	0.423	0.448	0.081	0.098	2.719	4.501	0.291
N3	0.195	0.189	0.427	0.422	0.488	0.045	0.099	3.324	5.189	0.289
N4	0.158	0.174	0.277	0.367	0.441	0.039	0.073	2.407	3.936	0.232
N5	0.192	0.259	0.515	0.592	0.930	0.126	0.178	4.644	7.435	0.442
N6	0.245	0.208	0.428	0.482	0.742	0.099	0.152	4.281	6.638	0.387
N7	0.260	0.220	0.416	0.489	0.814	0.072	0.143	4.626	7.040	0.382
N8	0.248	0.232	0.451	0.500	0.703	0.074	0.184	4.112	6.504	0.388
zone										0.282

Ecological risk factor and Potential ecological risk

Er values of El-Rayahs sediments showed that all sites have a low ecological risk for all analyzed metals, except Cd that showed moderate to considerable risk at RT, RM, and RN, with a noticeable increase northward; a high ecological risk exists in RB especially, at the northern segment (El-Mahmoudia Canal) (Table 5). In the same context, the potential ecological risk (RI) showed a low ecological risk for all Rayahs except the north of RB, which had a high ecological risk (Table 5).

Table (5): Ecological Risk Factor (Er), Potential Ecological Risk Index (RI) of the studied trace metals of the four Rayahs sediments.

Site	Ecological Risk Factor (Er)								Potential Ecological Risk Index (RI)
	Fe	Mn	Zn	Cu	Pb	Ni	Cr	Cd	
T1	0.144	0.130	0.172	0.620	1.204	0.262	0.074	42.125	44.73
T2	0.184	0.145	0.179	0.880	1.609	0.252	0.107	49.185	52.54
T3	0.210	0.144	0.183	1.034	1.833	0.237	0.126	57.910	61.68
T4	0.241	0.164	0.266	1.091	1.945	0.353	0.156	69.100	73.32
T5	0.229	0.178	0.273	1.140	1.859	0.309	0.134	74.208	78.33
T6	0.243	0.160	0.293	1.313	1.985	0.269	0.137	73.405	77.80
T7	0.325	0.212	0.383	1.585	3.226	0.413	0.195	126.450	132.79
M1	0.169	0.187	0.257	1.189	1.871	0.265	0.148	73.600	77.69
M2	0.174	0.205	0.219	1.231	1.764	0.282	0.140	72.350	76.37
M3	0.194	0.187	0.247	1.528	1.973	0.227	0.162	74.100	78.62
M4	0.291	0.265	0.439	2.064	3.976	0.499	0.246	114.400	122.18
M5	0.245	0.220	0.320	1.626	2.301	0.327	0.169	98.725	103.93
M6	0.248	0.194	0.336	1.662	2.702	0.301	0.174	99.225	104.84
M7	0.239	0.214	0.343	1.701	3.271	0.356	0.180	107.300	113.61
B1	0.167	0.299	0.702	2.706	2.588	0.283	0.371	78.450	85.57
B2	0.153	0.268	0.828	2.916	2.105	0.207	0.309	101.500	108.29
B3	0.177	0.267	0.762	2.502	2.035	0.175	0.315	100.880	107.11
B4	0.209	0.252	0.748	2.824	2.515	0.224	0.238	107.450	114.46
B5	0.176	0.307	0.666	3.299	2.241	0.249	0.455	100.375	107.77
B6	0.319	0.445	1.153	5.006	6.886	0.628	0.745	306.621	321.80
B7	0.276	0.378	0.886	4.038	5.310	0.430	0.565	232.140	244.02
B8	0.266	0.363	0.956	4.111	5.186	0.458	0.553	172.778	184.67
B9	0.298	0.416	1.114	4.536	6.258	0.542	0.656	255.275	269.10
N1	0.182	0.198	0.417	2.099	2.026	0.319	0.211	84.443	89.89
N2	0.181	0.192	0.359	2.116	2.238	0.405	0.197	81.575	87.26
N3	0.195	0.189	0.427	2.108	2.438	0.225	0.198	99.725	105.51
N4	0.158	0.174	0.277	1.835	2.207	0.194	0.147	72.200	77.19
N5	0.192	0.259	0.515	2.958	4.651	0.630	0.356	139.325	148.88
N6	0.245	0.208	0.428	2.410	3.709	0.495	0.304	128.425	136.23
N7	0.260	0.220	0.416	2.445	4.071	0.360	0.286	138.775	146.83
N8	0.248	0.232	0.451	2.502	3.516	0.371	0.368	123.350	131.04

Enrichment factor

The enrichment factor (EF) is a widely used measure for assessing the relative increase of metal compared to average natural abundance because of human activity. In the present study, Fe has been selected as the immobile element. Furthermore, ASVs levels are used as background concentrations; several authors indicated the degree of metal pollution with metal levels according to average shale (Muller, 1969; Forstner & Muller, 1973; Goher et al., 2014; Goher et al., 2021; Nasir et al., 2021).

According to Table 2, four contamination groups are commonly diagnosed based on the enrichment factor (Sutherland, 2000): EF > 1 indicates high metal content in the sample relative to its level in the Earth's crust. In contrast, EF values > 5 define sediments as polluted (Atgin et al., 2000). According to Zhang and Liu (2002), EF values between 0.5 and 1.5 suggest that the source of metals in sediments is because of crustal materials or natural processes, whereas EF values > 1.5 indicate an anthropogenic effect. Based on the above considerations, values of EF of Ni, Cr, and Mn did not cause remarkable contamination in the EI-Rayahs sediments; however, Cu and Zn in RB and RN, and Pb in all Rayahs, except RT, showed moderate contamination. Only Cd showed high EF values, indicating significant to very high enrichment at all EI-Rayahs, signifying the anthropogenic source of Cd (Table 6).

Table (6): Enrichment Factor (EF) of the studied trace metals of the four Rayahs sediments.

Site	Enrichment Factor (EF)							
	Fe	Mn	Zn	Cu	Pb	Ni	Cr	Cd
T1		0.897	1.193	0.858	1.668	0.362	0.258	9.721
T2		0.789	0.973	0.955	1.746	0.273	0.29	8.894
T3		0.687	0.875	0.986	1.747	0.226	0.3	9.204
T4		0.678	1.103	0.904	1.612	0.292	0.323	9.545
T5		0.78	1.194	0.998	1.626	0.27	0.294	10.82
T6		0.661	1.208	1.083	1.637	0.222	0.283	10.09
T7		0.654	1.178	0.976	1.986	0.254	0.3	12.98
M1		1.101	1.519	1.403	2.208	0.313	0.437	14.48
M2		1.177	1.255	1.412	2.023	0.323	0.4	13.83
M3		0.962	1.271	1.574	2.033	0.233	0.417	12.72
M4		0.91	1.505	1.417	2.729	0.342	0.422	13.09
M5		0.896	1.306	1.325	1.875	0.266	0.344	13.41
M6		0.785	1.355	1.342	2.181	0.243	0.352	13.35
M7		0.897	1.434	1.422	2.735	0.297	0.377	14.95
B1		1.794	4.206	3.243	3.102	0.339	1.113	15.67
B2		1.755	5.432	3.824	2.76	0.271	1.012	22.18
B3		1.509	4.3	2.822	2.295	0.197	0.887	18.96
B4		1.207	3.589	2.708	2.412	0.215	0.57	17.18
B5		1.744	3.791	3.754	2.55	0.284	1.295	19.03
B6		1.394	3.615	3.138	4.316	0.394	1.167	32.03
B7		1.366	3.205	2.922	3.843	0.311	1.023	28
B8		1.367	3.601	3.097	3.906	0.345	1.041	21.69
B9		1.398	3.739	3.046	4.203	0.364	1.101	28.57
N1		1.09	2.292	2.31	2.23	0.351	0.581	15.49
N2		1.061	1.983	2.336	2.472	0.447	0.543	15.02
N3		0.97	2.191	2.161	2.499	0.23	0.508	17.04
N4		1.104	1.758	2.328	2.8	0.246	0.466	15.27
N5		1.352	2.689	3.089	4.857	0.658	0.928	24.25
N6		0.849	1.744	1.964	3.022	0.403	0.619	17.44
N7		0.848	1.603	1.883	3.136	0.278	0.551	17.82
N8		0.938	1.821	2.02	2.839	0.299	0.742	16.6

Geo-accumulation index

Muller (1981) proposed seven grades (or classes) of the geo-accumulation index (Table 2). According to the I_{geo} of the analyzed metals (Table 7), El-Rayahs sediments are classified as unpolluted for all metals at all sites, except Cd, which exhibited moderate pollution in most sites, with a remarkable enrichment northward, particularly in RB.

Table (7): Index Geo-Accumulation (I_{geo}) of the studied trace metals of the four Rayahs sediments.

Site	Index Geo-Accumulation (I_{geo})							
	Fe	Mn	Zn	Cu	Pb	Ni	Cr	Cd
T1	-3.38	-3.53	-3.12	-3.597	-2.64	-4.84	-5.33	-0.1
T2	-3.02	-3.37	-3.06	-3.091	-2.22	-4.9	-4.81	0.128
T3	-2.84	-3.38	-3.03	-2.859	-2.03	-4.98	-4.57	0.364
T4	-2.64	-3.2	-2.49	-2.781	-1.95	-4.41	-4.26	0.619
T5	-2.71	-3.07	-2.46	-2.717	-2.01	-4.6	-4.48	0.722
T6	-2.63	-3.23	-2.36	-2.514	-1.92	-4.8	-4.45	0.706
T7	-2.21	-2.82	-1.97	-2.242	-1.22	-4.18	-3.94	1.491
M1	-3.15	-3.01	-2.54	-2.657	-2	-4.82	-4.34	0.71
M2	-3.1	-2.87	-2.78	-2.607	-2.09	-4.73	-4.43	0.685
M3	-2.95	-3.01	-2.6	-2.296	-1.93	-5.05	-4.21	0.72
M4	-2.36	-2.5	-1.77	-1.861	-0.92	-3.91	-3.61	1.346
M5	-2.61	-2.77	-2.23	-2.206	-1.7	-4.52	-4.15	1.133
M6	-2.6	-2.95	-2.16	-2.174	-1.47	-4.64	-4.1	1.141
M7	-2.65	-2.81	-2.13	-2.141	-1.2	-4.4	-4.06	1.254
B1	-3.17	-2.33	-1.1	-1.471	-1.54	-4.73	-3.01	0.802
B2	-3.3	-2.49	-0.86	-1.363	-1.83	-5.18	-3.28	1.173
B3	-3.08	-2.49	-0.98	-1.584	-1.88	-5.42	-3.25	1.165
B4	-2.85	-2.58	-1	-1.409	-1.58	-5.07	-3.66	1.256
B5	-3.09	-2.29	-1.17	-1.185	-1.74	-4.91	-2.72	1.157
B6	-2.23	-1.75	-0.38	-0.583	-0.12	-3.58	-2.01	2.768
B7	-2.44	-1.99	-0.76	-0.893	-0.5	-4.12	-2.41	2.367
B8	-2.5	-2.05	-0.65	-0.867	-0.53	-4.03	-2.44	1.941
B9	-2.33	-1.85	-0.43	-0.725	-0.26	-3.79	-2.19	2.504
N1	-3.05	-2.92	-1.85	-1.837	-1.89	-4.56	-3.83	0.908
N2	-3.05	-2.97	-2.06	-1.826	-1.74	-4.21	-3.93	0.858
N3	-2.94	-2.99	-1.81	-1.831	-1.62	-5.06	-3.92	1.148
N4	-3.25	-3.11	-2.44	-2.031	-1.76	-5.28	-4.35	0.682
N5	-2.97	-2.53	-1.54	-1.342	-0.69	-3.57	-3.08	1.63
N6	-2.61	-2.85	-1.81	-1.638	-1.02	-3.92	-3.3	1.513
N7	-2.53	-2.77	-1.85	-1.617	-0.88	-4.38	-3.39	1.625
N8	-2.6	-2.69	-1.73	-1.584	-1.09	-4.34	-3.03	1.455

Notably, based on different indices data, Cd represented the source of higher environmental risk in all El-Rayahs sediments, which is consistent with (Goher et al., 2021) for sediments of the Nile River from Aswan to Cairo. However, our results differ from (Abou El-Anwar, 2019), who indicated that Zn, Ni, Cr, and Cd are the most possible sources of pollution in sediments of Nile in Upper Egypt.

Sediment quality guidelines

In recent years, the effect of contaminated sediments on sediment-dwelling organisms (such as invertebrates and plants), aquatic-dependent wildlife (such as mammals, birds, fish, reptiles, and amphibians), and human health has become more intelligible. There are three levels of potential toxic effect on benthic creatures that depend on the continuous, long-term impact of pollutants: the first is “no effect levels,” at which no hazardous effect on aquatic creatures has been documented and where no biomagnification via food chain is anticipated; the second is the “lowest effect level,” which denotes a level of sediment pollution that the majority of benthic organisms can tolerate or at which the levels of contaminant exhibit a low possible risk effect; the third is the “severe effect level,” which denotes the levels of pollutant that has a high potential effect and may harm the majority of benthic species. Moreover, the sediment-dwelling community is likely to be significantly disrupted.

There are different approaches for the sediment quality guidelines set by several authors and organizations (Persaud et al., 1993; Smith et al., 1996; Long & Morgan, 1991; USEPA, 1996b, 1997; SLC/MENVIQ, 1992). In the present study, the screening level concentration approach (SLCA), recommended by (Persaud et al., 1993) for the lowest effect level (LEL) and severe effect level (SEL), is used to assess the quality of El-Rayahs sediments and the potential risk of HMs on benthic organisms. Table 8 shows that Fe, Mn, Zn, Ni, and Pb were below their LEL levels: thus, they did not have any adverse effect on benthic organisms in all El-Rayahs. However, Cd exceeded LEL in 47% of RT and all other sites, confirming that Cd has the greatest toxic effect on benthic creatures. Furthermore, Cu exceeded LEL and showed adverse effect in 14.3%, 100%, and 75%, in RM, RB, and RN samples, respectively, whereas Cr recorded values above its LEL in 100% of RB samples.

Table (8). The levels of heavy metals in El-Rayah sediment in µg/g (dry weight) compared to the levels of Sediment Quality Guidelines (SQGs)									
Metal		Cd	Cr	Cu	Fe ¹	Pb	Mn ¹	Ni	Zn
SQGs ⁽¹⁾	LEL	0.6	26	16	20000	31	460	16	120
	SEL	10	110	110	40000	250	1100	75	820
El-Tawfiky	present result	0.421–1.265	3.35–8.79	4.96–12.68	6750–15170	4.82–12.9	123.16–201.81	3.22–5.62	16.83–36.36
	Samples < LEL	%	43	100	100	100	100	100	100
	<SEL samples > LEL	%	57	0	0	0	0	0	0
	Samples > SEL	%	0	0	0	0	0	0	0
El-Menoufy	present result	0.724–1.144	6.28–11.08	9.51–16.51	7910–13610	7.06–15.9	177.2–252.04	3.08–6.78	20.8–41.66
	Samples < LEL	%	0	100	85.7	100	100	100	100
	<SEL samples > LEL	%	100	0	14.3	0	0	0	0
	Samples > SEL	%	0	0	0	0	0	0	0
El-Beahy	present result	0.785–3.056	10.7–33.5	20.02–40.05	7120–14900	8.14–27.54	239.14–422.5	2.38–8.54	7.12–109.56
	Samples < LEL	%	0	77.8	0	100	100	100	100
	<SEL samples > LEL	%	100	22.2	100	0	0	0	0
	Samples > SEL	%	0	0	0	0	0	0	0
El-Nassery	present result	0.722–1.393	6.61–16.54	14.68–23.66	7360–12130	8.11–18.6	165.29–245.96	2.63–8.57	26.33–48.93
	Samples < LEL	%	0	100	25	100	100	100	100
	<SEL samples > LEL	%	100	0	75	0	0	0	0
	Samples > SEL	%	0	0	0	0	0	0	0

SQG = Sediment Quality guidelines; LEL = lowest effect level; SEL = severe effect level; (1) according to Persaud et al., (1993),

Conclusions

The Nile River is the main source of water in Egypt, and human civilization has built around its banks since ancient times. The population gathers along it, especially in the study area (the Delta region). A crowded population lives around El-Rayahs and the Damietta and Rosetta branches, which provide fresh water to approximately 40 million people living in the Delta and Alexandria city. However, the Nile River and its canals are exposed to many sources of pollution because of the increase in human activities. Therefore, the present study aims to evaluate the levels and pollution degree of HMs in sediments of the four Rayahs (RT, RM, RB, RN) that can be used as a pollution indicator of the aquatic environment. Our study showed that more than 70% of El-Rayahs sediments were constituted by sand, with OM ranging from 4.48–16.47%. The absolute maximum values for most metals were found at RB, except Fe and Ni, recorded at RT and RN, respectively, whereas the minimum values were recorded at RT, except Ni recorded at RN with a remarkable increase in metals accumulation northward in all Rayahs. In general, indices data showed that the studied HMs did not cause significant ecological risk except Cd, which represented the highest possible environmental pollution. This finding was confirmed by the results of the SLCA of sediment quality criteria for the (LEL) and SEL. In addition, results of the integrated indices indicated that El-Rayahs were not polluted with HMs, except the northern part of RB (El-Mahmoudia Canal), which is classified as a highly-polluted area. Our research recommends the continuation of environmental monitoring of the four Rayahs and to enforce laws that prevent the dumping of waste in the waterways of the Nile River, especially RB and Rosetta branch (the source of water for El-Mahmoudia Canal).

Declarations

Data availability

All data will be available from the corresponding author upon request.

Statements and Declarations

Funding No funding was received for conducting this study.

Competing Interests The authors have no relevant financial or non-financial interests to disclose

Author contribution Field study and sampling, Seliem M. El-Sayed, Salem G. Salem, Mohamed E. Goher; Sample processing and analysis, Seliem M. El-Sayed, Salem G. Salem, Mohamed H. Abdo, Mohamed E. Goher; writing of the first draft and final text, Seliem M. El-Sayed, Salem G. Salem, Mohamed H. Abdo, Mohamed H.H. Ali, Mohamed E. Goher; review, editing and approving of the final text, Seliem M. El-Sayed, Salem G. Salem, Mohamed H. Abdo, Mohamed H.H. Ali, Mohamed E. Goher.

Ethical Approval Not applicable

Code availability Non applicable.

Consent to participate All authors voluntarily agree to participate in this research study.

Consent to publish All authors voluntarily approved the publication of this research study.

References

1. Abd El-Aal, F. I., El Sayed, S. M., Attia, M. S., Donia, N. S., Goher, M. E. (2020). Pollution indices and distribution pattern of heavy metals in Qarun Lake water, Egypt. *Egyptian Journal of Aquatic Biology & Fisheries*, 24(1): 593–607. DOI: 10.21608/EJABF.2020.75893
2. Abd El-Monsif, A. (2009). Mineral composition and environmental geochemical assessment of bottom sediments of main Nile course from Aswan to Isna "Upper Egypt". Ph. D. Thesis, Department of Geolog., Faculty of Science, Cairo University, 125.
3. Abdel-Satar, A. M (2005). Water quality assessment of River Nile from Idfo to Cairo. *Egypt. J. Aquat. Res.* 31 (2), 200–223.
4. Abou El-Anwar, E. A (2019). Assessment of heavy metal pollution in soil and bottom sediment of Upper Egypt: comparison study. *Bull Natl Res Cent* 43, 180. <https://doi.org/10.1186/s42269-019-0233-4>
5. Abou El-Anwar, E. A, Salman, S., Asmoay, A., Elnazzer, A. (2021). Geochemical, mineralogical and pollution assessment of River Nile sediments at Assiut Governorate, Egypt. *Journal of African Earth Sciences* 180, 104227. <https://doi.org/10.1016/j.jafrearsci.2021.104227>
6. Abu El-Enain, F. M, Lotfy, I. M, El-Sorogy, A. S, Wahid El-Din, A. M. (1997). Sedimentological, mineralogical and geochemical studies on the recent sediments of river Nile, near greater Cairo Egypt. *Egyptian Journal of Applied Sciences* 12 1028–1051.
7. Ahmed, A., Wal A., Bhattacharya, p., Genuchten, C. (2019). Characteristics of Fe and Mn bearing precipitates generated by Fe(II) and Mn(II) co-oxidation with O₂, MnO₄ and HOCl in the presence of groundwater ions, *Water Research*, 161, 505–516, <https://doi.org/10.1016/j.watres.2019.06.036>.
8. AIP (2017) AIP (American Institute of Physics) Conference Proceedings 1862, 030105, <https://doi.org/10.1063/1.4991209> Published Online: 10 July 2017
9. Alagarsamy, R. (2006). Distribution and seasonal variation of trace metals in surface sediments of the Mandovi estuary, west coast of India. *Estuarine, Coastal and Shelf Science* 67 333–339.
10. Ali, H., Khan, E., Ilahi, I. (2019). Environmental chemistry and ecotoxicology of hazardous heavy metals: Environmental persistence, toxicity, and bioaccumulation. *Journal of Chemistry*, 2019, 1–14. <https://doi.org/10.1155/2019/6730305>
11. Arefin, M. T, Rahman, M. M., Wahid-U-Zzaman, M., Kim, J. E. (2016). Heavy metal contamination in surface water used for irrigation: Functional assessment of the Turag river in Bangladesh. *J. Appl. Biol. Chem.*, 59, 83–90. <https://doi.org/10.3839/jabc.2016.015>
12. Atgin, R. S., El-Agha, O., Zararsiz, A., Kocatas, A., Parlak, H., Tuncel, G. (2000). Investigation of the sediment pollution in Izmir Bay: trace elements. *Spectrochim. Acta B* 55 (7), 1151–1164.
13. Bern, C. R., Katie Walton-Day, K., Naftz, D.L. (2019). Improved enrichment factor calculations through principal component analysis: Examples from soils near breccia pipe uranium mines, Arizona, USA, *Environmental Pollution*, (248): 90–100 <https://doi.org/10.1016/j.envpol.2019.01.122>.
14. Blaser, P, Zimmermann S., Luster J. (2000). Critical Examination of Trace Element Enrichments and Depletions in Soils: As, Cr, Cu, Ni, Pb, and Zn in Swiss Forest Soils. *The Science of the Total Environment*, 249: 257–280.
15. Bremner, L. (2021). Sedimentary Ways, *Geo Humanities*, 7:1, 24–43, <https://doi.org/10.1080/2373566X.2020.1799718>
16. Cabrera, F, Clemente, L, Barrientos, D. E. (1999). Heavy metal pollution of soils affected by the Guadamar toxic flood. *The Science of the Total Environment* 242 (1–3), 117–129.
17. Carver, R. E. (1971). *Procedures in Sedimentary Petrology*. John Wiley and Sons. Canada, Limited, New York, 653 p.
18. Chatterjee, M., Silva, F. E. V., Sarkar, S. K. (2007). Distribution and Possible Source of Trace Elements in the Sediment Cores of a Tropical Macrotidal Estuary and Their Ecotoxicological Significance. *Environment International*, 33: 346–356
19. Dianto, A., Ridwansyah, I., Subehi, L. (2020). Organic matter and organic carbon levels in sediments of Lake Maninjau, West Sumatra. *IOP Conf. Ser.: Earth Environ. Sci.* 535 012030. <https://doi.org/10.1088/1755-1315/535/1/012030>

20. Dinakaran, J., Krishnaya, N. S. R. (2011). Variations in total organic carbon and grain size distribution in ephemeral river sediments in western India. *International Journal of Sediment Research*, 26 (2): 239–246.
21. El Bouraie, M. M., El Barbary, A. A., Yehia, M. M., Motawea, E. A. (2011). Heavy metal concentrations in surface river water and bed sediments at Nile Delta in Egypt. *Suo* 61(1) 2010
22. El Sayed, S. M. (2015). Physico - chemical studies of water and sediment quality of Ismailia canal, River Nile, Egypt for its evaluation and protection from some hazard heavy metals Ph.D Thesis. Faculty of science, Al-Azher University, Egypt.
23. El-Amier, Y. A., El-kawy Zahran, M. A., Al-mamory, S. H. (2015). Assessment the Physicochemical Characteristics of Water and Sediment in Rosetta Branch, Egypt. *Journal of Water resource and Protection*, 7, 1075–1086.
24. El-Kammar, A. M., Ali, B. H., El-Badry, A. M. (2009). Environmental Geochemistry of River Nile Bottom Sediments Between Aswan and Isna, Upper Egypt. *Journal of Applied Sciences Research*, 5(6): 585–594, 2009
25. Elnazer, A. A., Mostafa, A., Salman, S. A., Seleem, E. M., Al-Gamal, A. G. (2018). Temporal and spatial evaluation of the River Nile water quality between Qena and Sohag Cities, Egypt. *Bull NRC* 42, 3. <https://doi.org/10.1186/s42269-018-0005-6>.
26. Elsherif, E. A., Badawi, A., Abdelkader, T. (2020). Grain size distribution and environmental implications of Rosetta beach, Mediterranean Sea coast, Egypt, *Egyptian Journal of Aquatic Biology & Fisheries*, ISSN 1110–6131. 24(1): 349–370.
27. Faraha, t H. I. (2019). Impact of Drain Effluent on Surficial Sediments in the Mediterranean Coastal Wetland: Sedimentological Characteristics and Metal Pollution Status at Lake Manzala, Egypt. *J. Ocean Univ. China* (Oceanic and Coastal Sea Research) ISSN 1672–5182, 2019 18 (4): 834–848. <https://doi.org/10.1007/s11802-019-3608-0>
28. Folk, R. L. (1980). *Petrology of Sedimentary Rocks*. Hemphills Publ Co, Austin, Texas, p. 170.
29. Forstner, U., Muller, G. (1973). **Heavy metal accumulation in river sediments: a response to environmental pollution.** *Geoforum* 145: 53–61.
30. Fu, J., Zhao, C., Luo, Y., Liu, C., Kyzas, G. Z., Luo, Y., Zhao, D., An, S., Zhu, H. (2014). Heavy metals in surface sediments of the Jialu River, China: their relations to environmental factors. *J Hazard Mater* 270:102–109. <https://doi.org/10.1016/j.jhazmat.2014.01.044>
31. Ghoneim E., Mashaly, J., Gamble, D., Halls, J., AbuBakr, M. (2015). Nile Delta exhibited a spatial reversal in the rates of shoreline retreat on the Rosetta promontory comparing pre-and post-beach protection. *Geomorphology*, 228: 1–14. Doi:10.1016/j.geomorph.2014.08.021
32. Goher, M. E. (1998). Factors affecting the precipitation and dissolution of some chemical elements in Nile River at Damietta Branch. M. Sci. Thesis, Fac. of Sci. Menofiya Univ. Egypt.
33. Goher, M. E. (2015). Monitoring of present environmental status of El-Rayahs, Nile River, Final Reports prepared to National Institute of Oceanography and Fisheries, Fresh Water and Lakes Division, Cairo, Egypt, 439 p.
34. Goher, M. E., Abdo, M. H., Mangood, A. H., Hussein, M. M. (2015). Water quality and potential health risk assessment for consumption of *Oreochromis niloticus* from El-Bahr El-Pharaony Drain, Egypt. *Fresenius Environ. Bull.* 24 (11): 3590–3602.
35. Goher, M. E., Ali, M. H. H., El Sayed, S. M. (2019). Heavy metals contents in Nasser Lake and the Nile River, Egypt: An overview, *Egyptian Journal of Aquatic Research*. 45 (4): 301–312. <https://doi.org/10.1016/j.ejar.2019.12.002>.
36. Goher, M. E., Farahat, H. I., Abdo, M. H., Salem, G. S. (2014). Metal pollution assessment in the surface sediment of Lake Nasser, Egypt. *Egyptian Journal of Aquatic Research*. 40(3), 225–233.
37. Goher, M. E., Mangood, A. H., Mousa, I. E., Salem, G. S., Hussein, M. M. (2021). Ecological risk assessment of heavy metal pollution in sediments of Nile River, Egypt. *Environ Monit Assess* 193:703 <https://doi.org/10.1007/s10661-021-09459-3>
38. Goldman, C. R. (2009). Micronutrient Elements (Co, Mo, Mn, Zn, Cu), Editor(s): Gene E. Likens, *Encyclopedia of Inland Waters*, Academic Press, 52–56, <https://doi.org/10.1016/B978-012370626-3.00094-6>
39. Griffiths, J. C. (1951). Size versus sorting in Caribbean sediments. *Jour.Geol.* 59, 211–243.
40. Hakanson, L. (1980). An ecological risk index for aquatic pollution control: a sedimentological approach. *Water Res.* 14, 975–1001.
41. Hamouda, A., El-Gharabawy, S., Awad, M., Shata, M., Badawi, A. (2014). Characteristic properties of seabed fluvial-marine sediments in front of Damietta promontory, Nile Delta, Egypt. *The Egyptian Journal of Aquatic Research*, 40(4): 373–383. Doi:10.1016/j.ejar.2014.11.006
42. Hanna, A. (1965). Organic matter in soil. In; *Chemistry of soil*. 2nd ed. Bear, E.F., Amre. Chem. Soc. Monography Series, N.Y.: 309–317.
43. Harikumar, P. S., Jishav T. S. (2010). Distribution pattern of trace metal pollutants in the sediments of an urban wetland in the Southwest Coast of India. *Int. J. Eng. Sci. Technol.* 2 (5), 840–850.
44. Huang, Z., Liu, C., Zhao, X. (2020). Risk assessment of heavy metals in the surface sediment at the drinking water source of the Xiangjiang River in South China. *Environ Sci Eur* 32, 23 (2020). <https://doi.org/10.1186/s12302-020-00305-w>
45. Imam, N., El-Sayed, S. M., Goher, M. E. (2020). Risk assessments and spatial distributions of natural radioactivity and heavy metals in Nasser Lake, Egypt. *Environ. Sci. Pollut. Res.* 27: 25475–25493. <https://doi.org/10.1007/s11356-020-08918-7>
46. Kabata-Pendias, H., Arun, B. M. (2007). *Trace Elements from Soil to Human*. ISBN-10 3-540-32713-4 Springer Berlin Heidelberg New York.
47. Karak, T., Kutu, F. R., Nath, J. R., Sonar, I., Paul, R. K., Boruah, R. K., Sanyal, S., Sabhapondit, S., Dutta, A. K. (2017). Micronutrients (B, Co, Cu, Fe, Mn, Mo, and Zn) content in made tea (*Camellia sinensis* L.) and tea infusion with health prospect: A critical review. *Crit Rev Food Sci Nutr.* 2017 Sep 22;57(14): 2996–3034. DOI: 10.1080/10408398.2015.1083534
48. Kouidri, M., Dali, youcef N., Benabdellah, I. et al., (2016). Enrichment and geoaccumulation of heavy metals and risk assessment of sediments from coast of Ain Temouchent (Algeria). *Arab J Geosci* 9, 354. <https://doi.org/10.1007/s12517-016-2377-y>

49. Lan, X. H., Zhang, Z. X., Li, R. H., Wang, Z. B., Chen, X. H., Hou, F. H. (2011). Geochemical characteristics of trace elements in the marine surface sediments outer Yangtze River Estuary. *Geoscience* 25 (6), 1066–1077.
50. Lasheen, M. R., Ammar, N. S. (2009). Speciation of some heavy metals in River Nile sediments, Cairo, Egypt. *Environmentalist* 29, 8–16. <https://doi.org/10.1007/s10669-008-9175-3>
51. Lenntech, (2022). **Nickel and water: reaction mechanisms, environmental impact and health effects. Available on line** <https://www.lenntech.com/periodic/water/nickel/nickel-and-water.htm#ixzz7fNPwoUdX>, last visit, 20/9/2022.
52. Lide, D. R. (2008). CRC Handbook of Chemistry and Physics, 88th edition 2007–2008. Boca Raton, Florida: Taylor & Francis Group, p. 4–71
53. Liu, W. H., Zhao, J. Z., Ouyang, Z. Y. (2005). **Impacts of Sewage Irrigation on Heavy Metal Distribution and Contamination in Beijing, China.** *Environment International*, 31: 805–812
54. Long, E. R., Morgan, L. G. (1991). The potential for biological effects of sediment-sorbed contaminants tested in the National Status and Trends Program. NOAA Technical Memorandum NOS OMA 52, National Oceanic and Atmospheric Administration, Seattle, WA, 175 pp 1 appendices.
55. Masoud, M. S., Fahmy, M. A., Ali, A. E. Mohamed, E. A. (2011). Heavy metal speciation and their accumulation in sediments of Lake Burullus, Egypt. *African Journal of Environmental Science and Technology* 5(4), 280–298.
56. Mateo-Sagasta, J., Zadeh, S. M., Turral, H. (2017). Water pollution from agriculture: a global review. Executive summary [Internet]. Rome, Italy: Food and Agriculture Organization of the United Nations (FAO); Colombo, Sri Lanka: International Water Management Institute (IWMI). <http://www.fao.org/3/a-i7754e.pdf>
57. Mohiuddin, K. M., Zakir, H. M., Otomo, K., Sharmin, S., Shikazono, N. (2010). Geochemical distribution of trace metal pollutants in water and sediments of downstream of an urban river. *Int. J. Environ. Sci. Technol.* 7 (1), 17–28.
58. Mostafa, A., Salman, S. A., Seleem, M. S., Elnazer, A. A., Al-Gamal, A. G., El-Taher, A., Mansour, H. (2019). Quality assessment of River Nile sediment between Qena and Sohag Cities, Egypt. *Jour Environ Sci Tech* 12 (3), 117–124. <https://doi.org/10.3923/jest.2019.117.124>.
59. Mucha, A. P., Vasconcelos M. T. S. D., Bordalo A. A. (2003). Macrobenthic community in the Doura estuary: relations with trace metals and natural sediment characteristics. *Environ. Pollut.* 121, 169–180.
60. Muller, G. (1969). **Index of geoaccumulation in sediments of the Rhine River.** *Geol. J.* 2: 109–118.
61. Muller, G. (1981). Die schwermetallbelastung der sedimente des neckars und seiner nebenflusse: eine estandsaufnahme. *Chem. Zeitung* 105,157–164.
62. Nasir, U., Saeed, M., Yousif, S. (2021). Environmental Impact Assessment of Heavy Metals in Surface Disposed Drilling Waste. *Journal of Geoscience and Environment Protection*, 9, 227–238. doi: 10.4236/gep.2021.99012.
63. Nielsen, F. (2021). **Nickel.** *Adv Nutr.* 1;12(1):281–282. doi: 10.1093/advances/nmaa154. PMID: 33307548; PMCID: PMC7849985.
64. Ottosen, L. M., Lepkova, K., Martin, K. (2006). Comparison of electro-dialytic removal of Cu from spiked kaolinite, spiked soil and industrially polluted soil. *Journal of Hazardous Materials* 137 113–120.
65. Paul, D. (2017). Research on heavy metal pollution of river Ganga: a review. *Ann. Agrar. Sci.* 15, 278–286. <https://doi.org/10.1016/j.aasci.2017.04.001>.
66. Persaud, D. R., Jaagumagi, R., Hayton, A. (1993). Guidelines for the Protection and Management of Aquatic Sediments in Ontario. Standards Development Branch. Ontario Ministry of Environment and Energy, Toronto, Canada, 27 pp.
67. Prashanth L., Kattapagari K. K., Chitturi R. T., Baddam, V. R. (2015). Prasad LK. A review on role of essential trace elements in health and disease. *J NTR Univ Health Sci*;4:75–85. DOI: 10.4103/2277-8632.158577
68. Qu, X., Ren, Z., Zhang, M. et al., (2017). Sediment heavy metals and benthic diversities in Hun-Tai River, northeast of China. *Environ Sci Pollut Res* 24, 10662–10673. <https://doi.org/10.1007/s11356-017-8642-0>
69. Raja, P, Achyuthan, H, Geethanjali, K, Chopra, S. (2018). **Late Pleistocene Paleoflood Deposits Identified by Grain Size Signatures, Parsons Valley Lake, Nilgiris, Tamil Nadu.** *J Geol Soc India* 91, 547–553. <https://doi.org/10.1007/s12594-018-0903-0>
70. RAMP (2021). Sediment quality, prepared by Regional Aquatics Monitoring Program (RAMP), available online <http://www.ramp-alberta.org/ramp/design+and+monitoring/components/sediment.aspx>. Last visit 12 October 2021
71. Salem, G. S. (2011). Sedimentary facies and geochemical studies on the recent bottom sediment of River Nile from Aswan to Cairo, Egypt. Ph.D. Thesis, Faculty of Science, Banha University, Egypt.
72. Salem, G. S. and Lotfy, M. H. (2017). Heavy Mineral Distribution and Geochemical Studies Of Damiatta And Rosseta Nile Branches, Egypt. *International Journal of Geology, Earth & Environmental Sciences* ISSN: 2277 – 2081.
73. SCDHEC (2020). A review of lead in surface waters Prepared by The Bureau of Water South Carolina Department of Health and Environmental Control, SCDHEC Technical Document Number: 003-2020, Available at: https://www.scdhec.gov/sites/default/files/media/document/final_Pb_report_w_annexes_jan_2020.pdf
74. Shyleshchandran, M. N., Mohan, M., Ramasamy, E. V. (2018). Risk assessment of heavy metals in Vembanad Lake sediments (south-west coast of India), based on acid-volatile sulfide (AVS)-simultaneously extracted metal (SEM) approach. *Environ Sci Pollut Res* 25, 7333–7345. <https://doi.org/10.1007/s11356-017-0997-8>
75. SLC/MENVIQ (ST. Lawrence Centre and Ministère de L'Environnement du Québec). (1992). Interim Criteria for Quality Assessment of St. Lawrence River Sediment. Environment Canada, Conservation and Protection, Quebec Region. Montréal
76. Smith, S. L., MacDonald, D. D., Keenleyside K. A., Ingersoll C. G., Field J. (1996). A preliminary evaluation of sediment quality assessment values for freshwater ecosystems. *J Great Lakes Res* 22:624–638.

77. Stanley, J. D., Goddio, F., Jorstad, T. F., Schnepf, G. (2004). Submergence of ancient Greek cities off Egypt's Nile Delta-A cautionary tale. *GSA TODAY*, 14(1): 4–10. Doi:10.1130/1052-5173(2004)014<4:SOAGCO>2.0.CO;2
78. Sutherland, R. A. (2000). Bed sediment-associated trace metals in an urban stream, Oahu, Hawaii. *Environ. Geol.* 39, 611–627.
79. Szarek-Gwiazda, E., Czaplicka-Kotas, A., Szalinska, E. (2011). **Background concentrations of nickel in the sediments of the carpathian dam reservoirs (Southern Poland),** *Clean - Soil Air Water*, 39 (2011) 368–375. <https://doi.org/10.1002/clen.201000114>
80. Talab A. S., Goher M. E., Ghannam H. E., Abdo M. H. (2016). Chemical compositions and heavy metal contents of *Oreochromis niloticus* from the main irrigated canals (Rayahs) of Nile Delta. *Egyptian Journal of Aquatic Research*, 42, 23–31.
81. Tiomo, I. F., Tematiov P., Momo, M. N., Happi, F. D., Guimapi, N. T., Tchaptchet, W. C. T. (2021). **Mineralogical and geochemical evolution of pre-lateritic soil profiles over schist basement of the Lom series (Bétaré-Oya, East Cameroon): Implication to rock weathering and lithologic constraints on trace elements fractionation,** *Journal of African Earth Sciences*, 176, 104133, <https://doi.org/10.1016/j.jafrearsci.2021.104133>.
82. Tomlinson, D. C., Wilson, J. G., Harris, C. R., Jeffrey, D. W. (1980). Problems in the assessment of heavy-metal levels in estuaries and the formation of a pollution index. *Helgoland Mar. Res.* 33, 566–575.
83. Tumolo, M., Ancona, V., De Paola, D., Losacco, D., Campanale C., Massarelli, C., Uricchio, V. F. (2020). Chromium Pollution in European Water, Sources, Health Risk, and Remediation Strategies: An Overview. *International journal of environmental research and public health*, 17(15), 5438. <https://doi.org/10.3390/ijerph17155438>
84. Turekian, K. K., Wedepohl, K. H. (1961). Distribution of the elements in some major units of the Earth's crust. *Geol. Soc. Am.* 72, 175–192.
85. UNCSO (2010). The United Nations Conference on Sustainable Development. New York, USA, May, 2010
86. USEPA (United States Environmental Protection Agency) (1996a). Microwave assisted acid digestion of siliceous and organically based matrices. SW-846 EPA Method 3052. Test Methods for Evaluating Solid Waste. 3rd Update. Washington, DC: US Environmental Protection Agency.
87. USEPA (United States Environmental Protection Agency) (1996b) Calculation and evaluation of sediment effect concentrations for the amphipod *Hyalella azteca* and the midge *Chironomus riparius*. EPA 905-R96-008, Great Lakes National Program Office, Region V, Chicago, IL
88. USEPA (United States Environmental Protection Agency) (1997). The incidence and severity of sediment contamination in surface waters of the United States. Volume 1: National sediment quality survey. EPA 823-R-97-006, Office of Science and Technology, Washington, DC.
89. Wani, A. L., Ara A., Usmani J. A. (2015). Lead toxicity: a review. *Interdisciplinary toxicology*, 8(2), 55–64. <https://doi.org/10.1515/intox-2015-0009>
90. Welte, D.H. (1969). **Organic Matter in Sediments.** In: Eglinton, G., Murphy, M.T.J. (eds) **Organic Geochemistry.** Springer, Berlin, Heidelberg. https://doi.org/10.1007/978-3-642-87734-6_12
91. WWAP (2017). The United Nations World Water Development Report 2017: Wastewater, the untapped resource. United Nations World Water Assessment Programme (WWAP). Paris, United Nations Educational, Scientific and Cultural Organization. https://www.unido.org/sites/default/files/2017-03/UN_World_Water_Development_Report_-_Full_0.pdf
92. Yuana, S., Tanga, H., Xiaoa, Y., Xiab, Y., Melchingcv C., Lia, Z. (2019). Phosphorus contamination of the surface sediment at a river confluence. *J. Hydrol.* 573, 568–580.
93. Zakir, H. M., Shikazono, N., Otomo, K. (2008). Geochemical distribution of trace metals and assessment of anthropogenic pollution in sediments of Old Nakagawa River, Tokyo. *Jpn. Am. J. Environ. Sci.* 4 (6), 661–672.
94. Zhang, J., Liu, C. L. (2002). Riverine composition and estuarine geochemistry of particulate metals in China-Weathering features, anthropogenic impact and chemical fluxes. *Estuar. Coast. Shelf Sci.* 54 (6), 1051–1070.
95. Zhang, L. P., Ye, X., Feng, H. (2007). **Heavy Metal Contamination in Western Xiamen Bay Sediments and Its Vicinity, China.** *Marine Pollution Bulletin*, 54: 974–982.

Figures

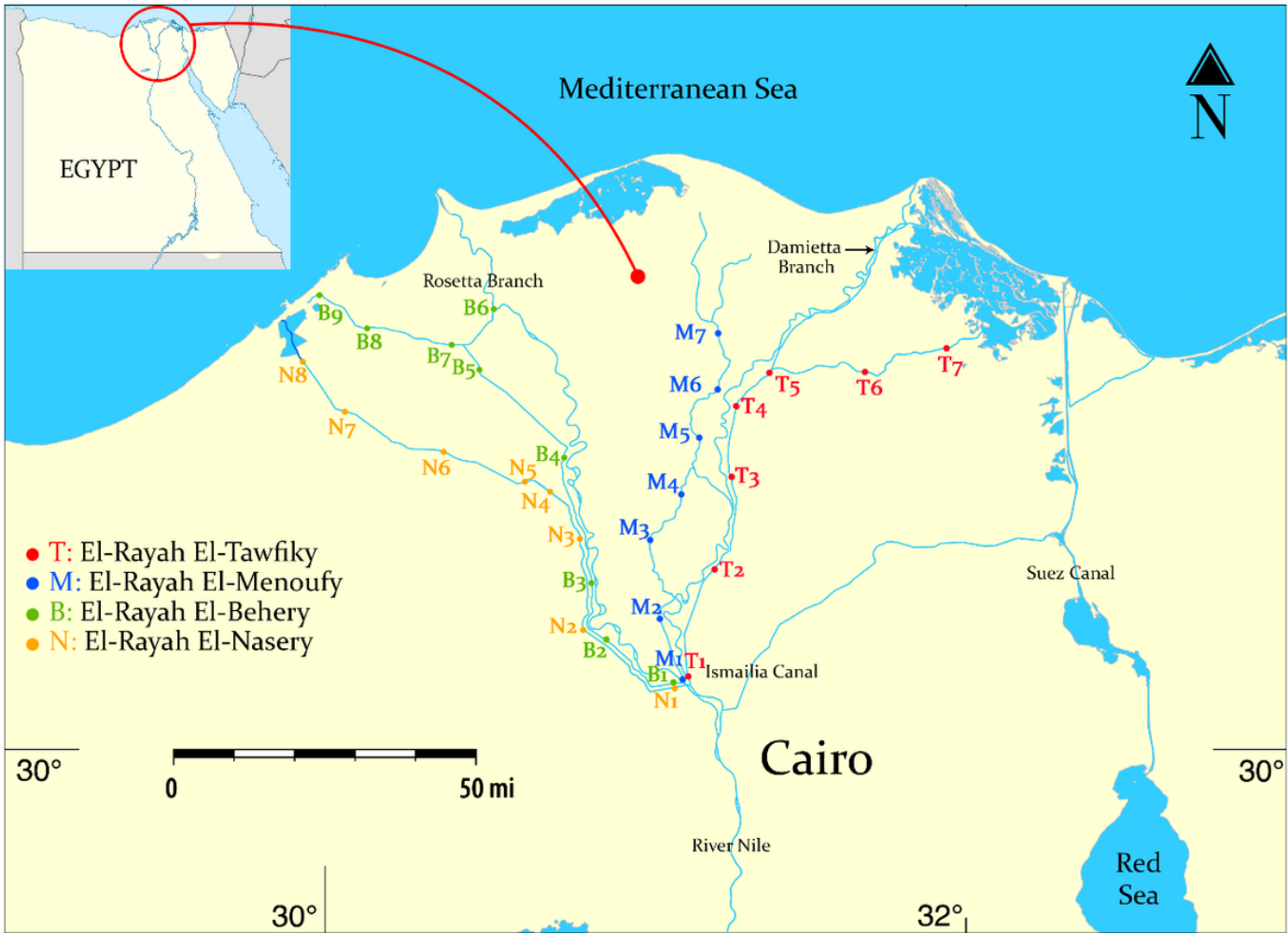


Figure 1
Map of the study area indicating the selecting sites

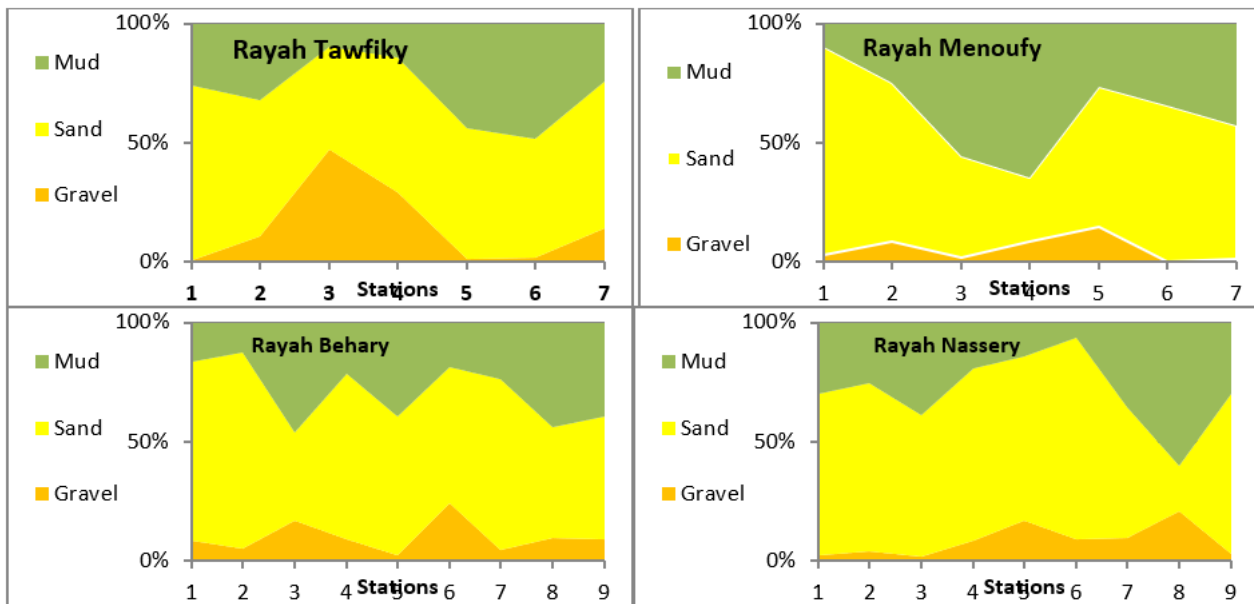


Figure 2
Horizontal distribution of grain size of the four Rayahs sediments.

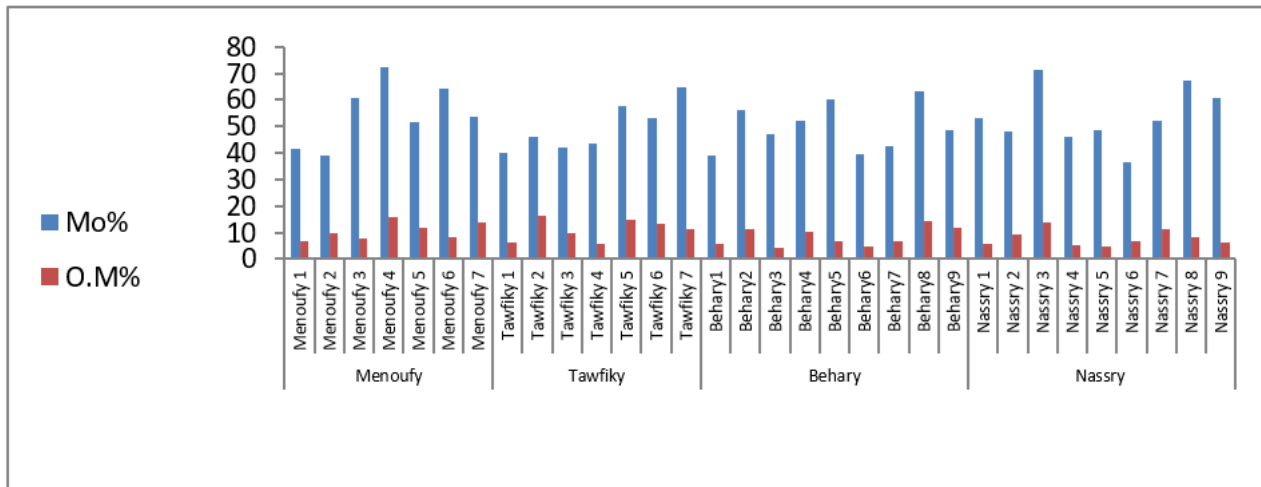


Figure 3

Organic matter and Moisture of the studied trace metals of the four Rayahs sediments

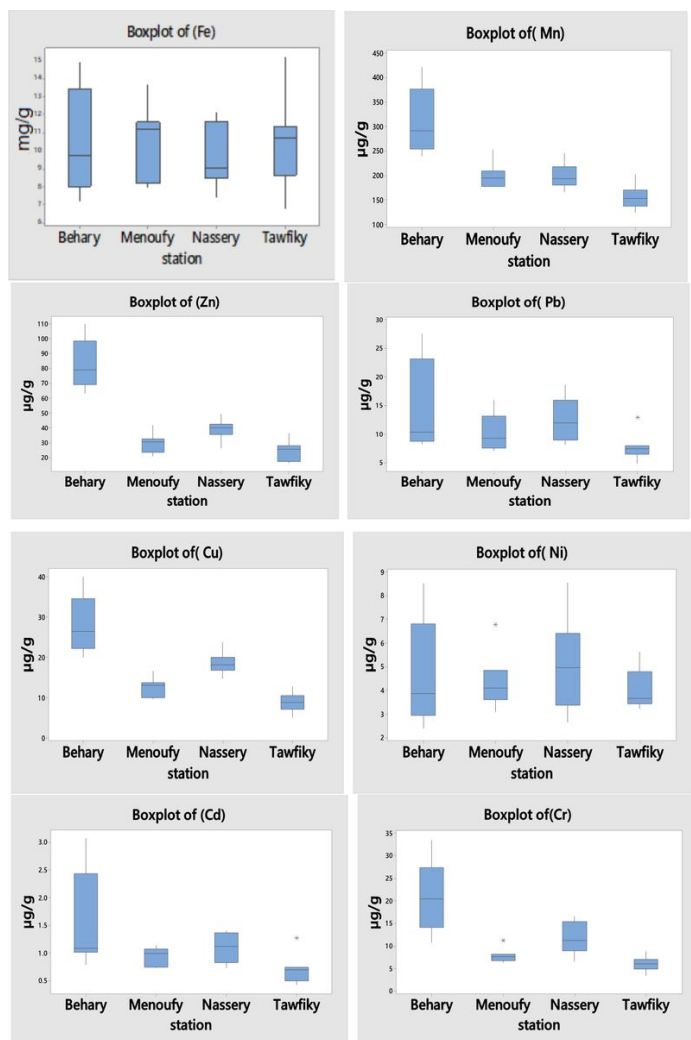


Figure 4

Box plot of the studied trace metals in the sediment of the four Rayahs.